IMPEDANCE CALCULATION AND SIMULATION OF MICROWAVE INSTABILITY FOR THE MAIN RINGS OF SUPERKEKB

T. Abe, T. Ishibashi, Y. Morita, K. Ohmi, K. Shibata, Y. Suetsugu, M. Tobiyama, D. Zhou*
KEK, 1-1 Oho, Tsukuba, Ibaraki 305-0801, Japan

Abstract

The SuperKEKB B-factory is now under construction. The designs of the components for the SuperKEKB have mostly been finished. This paper summarises the updated results of longitudinal impedance calculations for various components of the main rings. By summing up all available impedances, a pseudo-Green wake function with bunch length of σ_z=0.5 mm is constructed as an impedance model for consequent studies of collective effects. The results of these studies are also reported in this paper.

INTRODUCTION

The SuperKEKB B-factory is an upgrade of the KEKB. Most of the vacuum components in the low energy ring (LER) are replaced by new ones [1]. The new components are designed with criteria of minimising their impedances to avoid beam instabilities and reduce HOM heating. Several mitigation schemes are adopted to suppress the electron cloud effect [2], but affecting the impedance budget: 1) The round beam pipes of 45-mm radius with antechambers (see Fig. 1) are used for about 90% in total length of the LER. 2) The grooved surface is adopted for beam pipes in the bending magnets in the arc sections. 3) The clearing electrodes are used in wiggler magnets. 4) Almost all the beam pipes are coated with TiN.

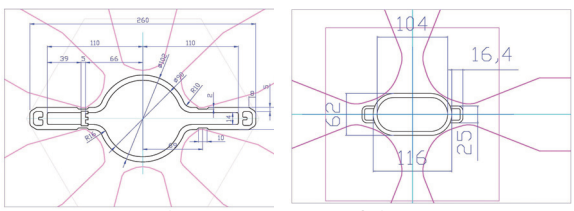

Figure 1: Typical cross-section of beam pipes in SuperKEKB. Left: LER with antechamber at arc sections in a sextuple magnet. Right: HER with race-track shape at the arc sections in a quadrupole magnet.

The high energy ring (HER) inherits most of the vacuum components from the HER of KEKB. The beam pipes are mostly reused and have race-track cross-section without antechamber (see Fig. 1), which occupies about 70% in total length of the HER. The full width and height of race-track pipes are 104 mm and 50 mm, respectively.

In this paper, the most recent impedance results from numerical calculations of the vacuum components in SuperKEKB are collected and converted to a pseudo-Green wake function. Then the data are used as inputs of the Vlasov-Fokker-Planck (VFP) solver code [3, 4] to perform simulations and predict the bunch lengthening and the microwave instability (MWI) threshold.

IMPEDANCE CALCULATION

For most of the vacuum components, the electromagnetic code GdfidL [5] is used for impedance calculations. A Gaussian bunch with σ_z=0.5 mm is chosen as the driving beam to obtain the Pseudo-Green wake function. With suitable approximations, the 2D ABCI code [6] is used to calculate the impedance of superconducting (SC) cavities instead of GdfidL. For the impedances of coherent synchrotron radiation (CSR) and coherent wiggler radiation (CWR), the code CSRZ [7] is used. For the resistive wall impedance, the analytical formulae [8] are used. For more detailed descriptions of the vacuum system and impedance issues, the readers are referred to Ref. [1, 2].

LER

To estimate the resistive wall impedance, the beam pipes are assumed be to aluminium with round shape of 45-mm radius. The bellows in the LER have comb-type RF shielding structure, which shows higher thermal strength and lower impedance compared with that of KEKB LER [2]. For the calculation of CSR impedance, the single-bend model is assumed, with conditions of: 1) bending radius 74.68 m; 2) magnet length 4.19 m; 3) square chamber cross-section with full width 90 mm. The wigglers in the LER have minimum bending radius of around 15 m, wavelength of 1.1 m, and about 300 periods in total.

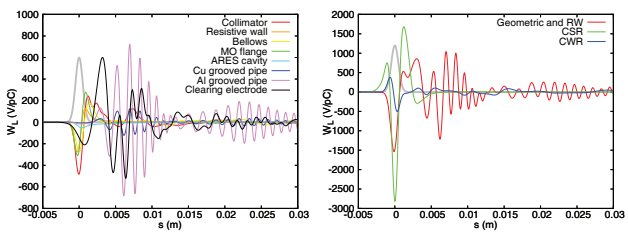

Figure 2: The wakes for important impedance sources with driving Gaussian bunch of σ_z=0.5 mm in LER. The grey line indicates the bunch profile. Left: Wakes of various components. Right: The total geometric and resistive wall wakes compared with CSR and CWR wakes.

Figure 2 shows the wakes of 0.5-mm Gaussian bunch for the important impedance sources in the LER. By convoluting the short-bunch wakes over the nominal bunch distribution, the long-bunch wakes are obtained as shown in Fig. 3. Since the pumping ports and synchrotron radiation (SR) masks are located inside the antechambers, their contributions to the impedance budget are negligible and not plotted in these figures. Other contributions from the duct in the interaction

* dmzhou@post.kek.jp

region (IR), the beam position monitors (BPM), the transverse feedback (FB) kickers, FB BPMs, and the longitudinal FB kicker are also not shown, but taken into account in the impedance budget.

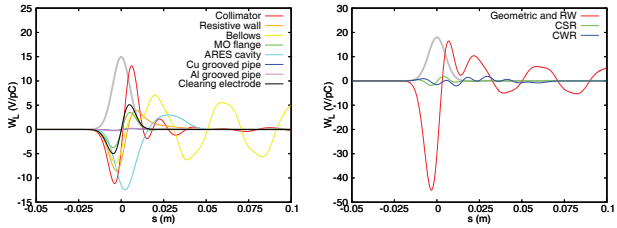

Figure 3: The wakes for important impedance sources with nominal Gaussian bunch of σ_z=5 mm in LER. Left: Wakes of various components. Right: The total geometric and resistive wall wakes compared with CSR and CWR wakes.

From the calculated wakes, it is seen that the CSR and CWR impedances have large amplitudes for short bunches, but almost negligible for long and smooth bunches. The importance of CSR and CWR lies in determining the MWI threshold as to be discussed in next section. Therefore, we alway add them to the impedance model for the whole ring. The wakes of collimators (or movable masks), flanges and clearing electrodes for nominal bunch length are nearly proportional to the derivative of the bunch profile, indicating that their impedance are inductive. There is trapped mode at frequency around 7.5 GHz in the comb-type bellows, and it leads to the oscillating structure in its wake.

HER

To estimate the resistive wall impedance, the beam pipes are assumed be to copper with round shape of 25-mm radius. For the CSR impedance calculation, the single-bend model is assumed, with conditions of: 1) bending radius 106 m; 2) magnet length 5.9 m; 3) rectangular chamber cross-section with full width 104 mm and full height 50 mm. The wiggler radiation impedance is not considered at present.

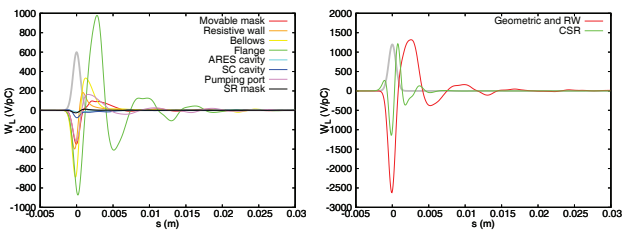

Figure 4: The wakes for important impedance sources with driving Gaussian bunch of σ_z=0.5 mm in HER. Left: Wakes of various components. Right: The total geometric and resistive wall wakes compared with CSR wake.

Figures 4 and 5 shows the wakes of 0.5- and 4.9-mm bunches for the important impedance sources in the HER. Since there is no antechamber in most of this ring, the pumping ports and SR masks contribute remarkable impedances to the budget. Contributions from IR duct, BPMs, FB kicker, and FB BPMs are not shown in the figures.

From the calculated wakes, it is seen that the CSR impedance in the HER is much weaker than that in the LER.

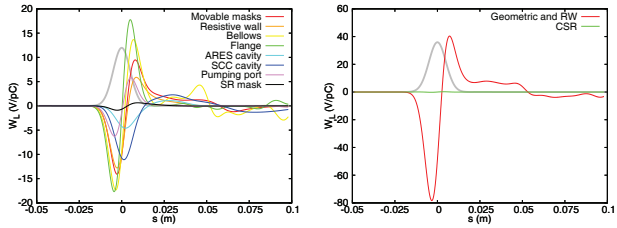

Figure 5: The wakes for important impedance sources with nominal Gaussian bunch of σ_z=4.9 mm in HER. Left: Wakes of various components. Right: The total geometric and resistive wall wakes compared with CSR wake.

This is due to the facts of longer bending radius and stronger chamber shielding. The wakes of movable masks, bellows, flanges, pumping ports and SR masks are mainly inductive.

Table 1: Impedance budget for the SuperKEKB main rings. Summarised are the contributions to the loss factor $k_{||}$ [V/pC], the fitted resistance R [Ω] and inductance L [nH] for each type of components. The resistances and inductances are calculated at the nominal bunch lengths of σ_z=5 and 4.9 mm for LER and HER, respectively.

Component	LER			HER		
	$k_{\|\|}$	R	L	$k_{\|\|}$	R	L
ARES cavity	8.9	524	-	3.3	190	-
SC cavity	-	-	-	7.8	454	-
Collimator	1.1	62.4	13.0	5.3	309	10.8
Res. wall	3.9	231	5.7	5.9	340	8.2
Bellows	2.7	159	5.1	4.6	265	16.0
Flange	0.2	13.7	4.1	0.6	34.1	19.3
Pump. port	0.0	0.0	0.0	0.6	34.1	6.6
SR mask	0.0	0.0	0.0	0.4	21.4	0.7
IR duct	0.0	2.2	0.5	0.0	2.2	0.5
BPM	0.1	8.2	0.6	0.0	0.0	0.0
FB kicker	0.4	26.3	0.0	0.5	26.2	0.0
FB BPM	0.0	1.1	0.0	0.0	1.1	0.0
Long. kicker	1.8	105	1.2	-	-	-
Groove pipe	0.1	3.8	0.5	-	-	-
Electrode	0.0	0.7	5.7	-	-	-
Total	19.2	1137	36.4	29.0	1677	62.1

Impedance Budget

The contributions from the geometric structures and resistive wall to the ring's impedance budget are summarised in Table 1. In the table, the loss factor $k_{||}$, resistance R and inductance L are calculated based on the wakes at nominal bunch lengths. Following Ref. [9], the R and L parameters are obtained by fitting the wakes using an analytical model. It is seen that: 1) for the LER, the dominant sources of inductance are collimators, resistive wall, bellows, clearing electrodes and flanges; 2) for the HER, the dominant sources of inductance are movable masks, resistive wall, bellows, flanges, and pumping ports.

MICROWAVE INSTABILITY

The main parameters used in the MWI simulations are listed in Table 2. Using the obtained Pseudo-Green wake

ISBN 978-3-95450-132-8

functions obtained in the previous section, the normalised bunch length and energy spread as a function of bunch population simulated by the VFP solver are presented in Figs. 6 and 7. Several inputs of impedance model are tested in the simulations. For all simulations, the maximum values of $|q|$ and $|p|$ as defined in Ref. [4] are 8, with 500 mesh points in each direction.

Table 2: Key Parameters of SuperKEKB Main Rings for MWI Simulations

Parameter	LER	HER
Circumference (m)	3016.25	3016.25
Beam energy (GeV)	4	7.007
Bunch population (10^{10})	9.04	6.53
Nominal bunch length (mm)	5	4.9
Synchrotron tune	0.0244	0.028
Long. damping time (ms)	21.6	29.0
Energy spread (10^{-4})	8.1	6.37

The simulations of MWI with CSR impedance are very tricky [4, 10]. In our simulations, the CSR impedance is treated as normal geometric wakes. The convolution of CSR impedance over 0.5-mm bunch surely suppresses the effect of impedance from very high frequencies. This might explain our simulated CSR thresholds are much higher that predicted by the formulae in Refs. [4, 11]. Below the MWI threshold, the CSR/CWR is too weak (see Figs. 3 and 5) to cause additional bunch lengthening over normal wakes.

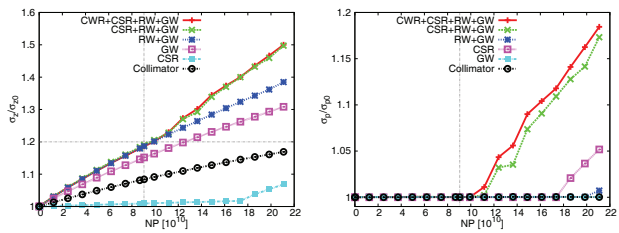

Figure 6: Normalised bunch length and energy spread as a function of the bunch population in LER. The vertical and horizontal dashed grey lines indicate the nominal bunch population and bunch length, respectively. Simulations are performed by using VFP solver with various impedance sources. Left: Bunch length. Right: Energy spread.

It is seen that the positron and electron beams have similar bunch-lengthening rate with all the impedance sources considered. The predicted bunch lengths at the nominal bunch population are 5.9 and 5.8 mm, respectively for the LER and HER. The detected MWI thresholds for the bunch population are around $N_{th}^{e+} = 1.05 \times 10^{11}$ and $N_{th}^{e-} = 1.7 \times 10^{11}$ correspondingly. They are considerably higher than the nominal values as shown in Table 2.

For the LER, the collimators are the most important impedance sources for the bunch lengthening. This is because that small gaps are necessary to secure the background control of the particle detector [12]. It is shown that the interplay between CSR/CWR and normal wakes causes significant reduction of MWI threshold. Its mechanism is not well understood yet. CSR causes additional bunch lengthening at bunch population above the MWI threshold, because microbunching will happen and hence amplify the CSR forces.

For the HER, bellows and flanges are more important than movable masks in causing bunch lengthening. The CSR does not cause increase in bunch length or energy spread for bunch population up to 2.4×10^{11}.

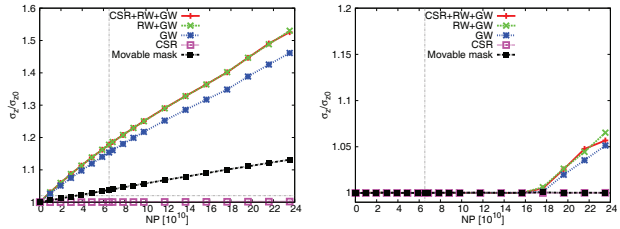

Figure 7: Normalised bunch length and energy spread as a function of the bunch population in HER. The vertical and horizontal dashed grey lines indicate the nominal bunch population and bunch length, respectively. Left: Bunch length. Right: Energy spread.

SUMMARY AND DISCUSSION

The longitudinal impedance models for the main rings of SuperKEKB are successfully constructed. The impedance budget for various impedance sources are also obtained. VFP simulations show that the bunch lengthening are less than 20% at nominal beam currents.

More efforts will be put on: 1) updates of the impedance models periodically; 2) preparations for impedance related measurements during the beam commissioning. Our simulations show that the main rings are safe from CSR instability, but this is not consistent with the predictions in Ref. [11]. It implies that more careful studies should be done to address the CSR effect in SuperKEKB.

The author D.Z. would like to thank Y. Cai and G. Stupakov for providing their VFP code and helpful discussions.

REFERENCES

[1] *SuperKEKB Technical Design Report*, To be published.

[2] Y. Suetsugu et al., J. Vac. Sci. Technol. A 30, 031602 (2012).

[3] Y. Cai et al., Phys. Rev. ST Accel. Beams 12, 061002 (2009).

[4] K. Bane et al., Phys. Rev. ST Accel. Beams 13, 104402 (2010).

[5] GdfidL website: `http://www.gdfidl.de/`

[6] ABCI website: `http://abci.kek.jp/`

[7] D. Zhou et al., Jpn. J. Appl. Phys. 51 (2012) 016401.

[8] A. Chao et al., *Handbook of Accelerator Physics and Engineering*, (Singapore : World Scientific, 2013), p.253.

[9] K. Bane et al., SLAC-PUB-13999, April 2010.

[10] L. Wang et al., IPAC'13, Shanghai, China, TUPME017 (2013).

[11] Y. Cai et al., Phys. Rev. ST Accel. Beams 17, 020702 (2014).

[12] H. Nakayama et al., IPAC'12, New Orleans, Louisiana, USA, TUOBC02 (2012).